

# STABILITY CRITERION FOR TWO-PHASE TRANSPIRATION COOLING

V. A. Maiorov and L. L. Vasil'ev

UDC 532.546

The stability criterion is established for two-phase transpiration cooling with phase-transition equilibrium inside the porous wall.

As an effective method of thermal protection, one now widely recommends the use of liquids which evaporate inside the cooled wall. Two-phase cooling offers some excellent features: a high absorption capacity of the coolant, which is due to evaporation of the liquid and the subsequent superheating of the generated vapor; there is no limitation here on the thermal flux density and on the shearing stresses at the outer surface; the discharging superheated vapor alters the temperature distribution in the outer boundary layer to such an extent that convective heat transfer to the surface abates appreciably; a temperature rise, within permissible limits, at the outer surface does further reduce the convection of heat and causes some of the heat to be dissipated into the ambient space by radiation.

Despite these obvious advantages, such a cooling system has so far remained completely unexplored. The reason for this is not a lack of research activity, but that, as experiments have revealed, a process with phase transformation inside a cooled wall is unstable [1-6].

Among all thermotechnical devices, those with phase transformation of the active medium are most prone to unstable operation whenever a small perturbation of the process parameters induces a transition of the system from one state to a very different other state [9-13]. Best known are such types of aperiodical instabilities in thermotechnical devices as critical boiling modes and sudden wide fluctuations in the flow rate of the active medium in the hot piping system of parallel-flow boilers.

In an unstable two-phase cooling system it is impossible for the boiling zone inside the porous wall to stabilize. A result of a higher heat load is that the stream of liquid which evaporates at the surface becomes replaced by a stream of vapor. The flow rate of coolant under constant feed pressure decreases fast and, under heavy heat loads, this is accompanied by a burning of the wall.

Instability under operating conditions typical of most experimental transpirators basically alters the system performance and gives rise to new dominant phenomena. We still have found no explanation for the essential characteristics of the stable process here and for the way in which various parameters affect them. According to the published evidence, two stable two-phase cooling systems have been so far developed successfully [6-8]. In both systems the stability is attained by the use of a multilayer porous structure, but ideas concerning the necessary properties of individual layers are vague. As to the effect of other parameters on the process stability, the authors of [7] have made some general assumptions which are valid for all two-phase systems.

The lack of necessary data pertaining to the basic trends of the stable process here makes a thorough mathematical description and subsequent computer-aided analysis impossible.

A logical way out of this stalemate is to develop a model which would simplify the actual process but retain all its qualitative characteristics. An analysis of such a model would reveal the main causes of instability in two-phase transpiration cooling. The authors have undertaken to determine the conditions which cause instability in two-phase transpiration cooling.

---

Institute of Heat and Mass Transfer, Academy of Sciences of the BSSR, Minsk. Translated from *Inzhenerno-Fizicheskii Zhurnal*, Vol. 25, No. 2, pp. 237-248, August, 1973. Original article submitted February 2, 1973.

© 1975 Plenum Publishing Corporation, 227 West 17th Street, New York, N.Y. 10011. No part of this publication may be reproduced, stored in a retrieval system, or transmitted, in any form or by any means, electronic, mechanical, photocopying, microfilming, recording or otherwise, without written permission of the publisher. A copy of this article is available from the publisher for \$19.00.

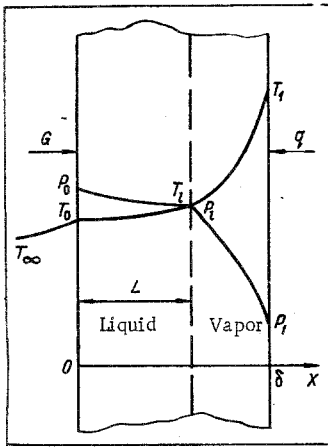


Fig. 1. Physical model of two-phase transpiration cooling.

The physical model of steady two-phase transpiration cooling is shown in Fig. 1. A homogeneous plane porous plate, very long and very wide relative to its thickness  $\delta$ , is exposed to an outside thermal flux of constant density  $q$ . The coolant is a liquid at an initial temperature  $T_\infty$ . Under a constant feed pressure  $P_0$ , this liquid is oozed into the ambient medium where a given pressure  $P_1$  prevails. While flowing through the porous wall, the liquid absorbs heat and its temperature rises so that the local temperatures of liquid coolant and wall material remain equal. Meanwhile, the pressure in the liquid decreases. As soon as the coolant temperature and pressure reach levels corresponding to saturation, there occurs a phase transformation. Boiling is confined to a thin (relative to the plate thickness) zone at a distance  $L$  from the inner surface. The generated vapor absorbs heat from the region between the boiling zone and the outer surface, whereupon, superheated, it discharges into the ambient space.

On the basis of this hypothetical mechanism, two-phase transpiration cooling can be described by a system of differential equations which includes:

the continuity equation

$$\frac{dG}{dX} = 0, \quad (1)$$

the flow equation

$$-\frac{dP}{dX} = \frac{\alpha\mu}{\rho} G + \frac{\beta}{\rho} G^2 \quad (2)$$

the energy equation

$$\lambda' \frac{d^2 t_0}{dX^2} - Gc' \frac{dt_0}{dX} = 0 \quad (3)$$

for the liquid region  $0 \geq X > -\infty$

$$\lambda_1 \frac{d^2 t_1}{dX^2} - Gc' \frac{dt_1}{dX} = 0 \quad (4)$$

for the porous-solid zone with liquid  $0 \leq X \leq L$

$$\lambda_2 \frac{d^2 t_2}{dX^2} - Gc'' \frac{dt_2}{dX} = 0 \quad (5)$$

and for the porous-solid zone with vapor  $L \leq X \leq \delta$ .

The boundary conditions represent the following aspects of the process: the initial temperature of the liquid is stipulated as

$$x = -\infty \quad t_0 = T_\infty; \quad (6)$$

At the inner surface the temperature and the thermal flux remain continuous:

$$X = 0 \quad t_0 = t_1 = T_0, \quad \lambda' \frac{dt_0}{dX} = \lambda_1 \frac{dt_1}{dX}; \quad (7)$$

At the phase-transition boundary the temperature distribution is continuous but the thermal flux changes by an amount necessary for complete evaporation of the liquid:

$$X = L \quad t_1 = t_2 = T_1, \quad \lambda_2 \frac{dt_2}{dX} - \lambda_1 \frac{dt_1}{dX} = Gr; \quad (8)$$

At the outer surface the thermal flux density, the ambient pressure, and the maximum temperature at which the plate material can still perform reliably are all defined:

$$X = \delta \quad q = \lambda_2 \frac{dt_2}{dX}, \quad P = P_1, \quad T_1 \leq T_1^*; \quad (9)$$

The location of the phase-transition boundary is found from the condition of equilibrium boiling:

$$X = L P_l = P_s(T_l). \quad (10)$$

and this makes the system of equations for our problem closed.

In writing the boundary conditions, we have denoted the unknown temperatures at the three surfaces by  $T_0$ ,  $T_l$ , and  $T_1$  respectively. The maximum permissible temperature at the outer surface  $T_1^*$  represents the boundary condition for integrating the continuity equation. For the second-order differential equations of energy, it is necessary to stipulate two boundary conditions: the density of the thermal flux from outside and the initial coolant temperature. At the interfaces one must satisfy the respective compatibility conditions. The parameters which govern the design of a cooling system are the loading thermal flux density and the ambient pressure as well as the kind of coolant substance and its initial temperature. We must now select a porous wall with characteristics which will ensure that its surface temperature does not exceed the permissible limit specified for reliable performance, with a minimum possible coolant flow rate and at as small as possible fluctuations of the other governing parameters. Furthermore, the feed pressure, the mass flow rate of coolant, and the location of the boiling zone inside the wall are also to be determined.

The modified Darcy equation (2) accounts for frictional drag (first term on the right-hand side) and for inertial drag (second term on the right-hand side) during the flow of a liquid through a porous medium. The drag coefficients (viscous friction  $\alpha$  and inertial drag  $\beta$ ) characterize a porous structure and do not depend on the kind of the filtrating liquid [14, 15], nor on the temperature of the material [15-18]. Only structural changes in the porous material which occur at high temperatures will alter its hydrodynamic characteristics [17].

Most effective for cooling systems are metal-ceramic materials produced from metal powder by compacting and then sintering. The drag coefficients in such materials are determined by their porosity as well as by the shape and the size of the original powder grains. Many data are available on the correlation between the porosity and the drag coefficients for various metal ceramics, and modern technology is capable of producing porous structures to meet specified hydrodynamic characteristics [18-23]. The effective thermal conductivity of two-phase systems (liquid in porous solid, vapor in porous solid) generally depends rather intricately on the structure and on the kind of porous material, also on the properties of the filler liquid [24]. The following simplest expressions will be adequate for a qualitative analysis

$$\lambda_1 = \lambda_m(1 - \Pi) + \lambda' \Pi; \quad \lambda_2 = \lambda_m(1 - \Pi) + \lambda'' \Pi. \quad (11)$$

A closer look at expressions (1)-(10) will reveal that this model of two-phase transpiration cooling is described by a nonlinear closed system of differential equations. The physical properties of the coolant which appear in the flow equation and in the energy equation are functions of both the temperature and the pressure, they also change stepwise during phase transformation. The location of the phase-transition boundary is, in turn, found by solving these equations on the premise that a phase transformation and a change in thermal flux at the sought boundary are equivalent. Finally, the coolant flow rate is also one of the unknown quantities here.

A problem like this can be solved only by a numerical method. Such a method will not yield the most important answer, however, namely the range within which the parameters may vary without exceeding the limits of stable performance. In this case, when the actual cooling process becomes unstable, it is oscillatory and quite different from the theoretical process calculated with the same nominal values of the system parameters [25].

A derivation of the stability criterion requires a more general approach but, at the same time, our proposed method of analysis is more thorough and more economical in terms of computation time. If the location of the phase-transition boundary is assumed known, then the flow equation and the energy equation will yield the pressure and the temperature at that hypothetical phase-transition boundary. These values of pressure and temperature can then be represented by a point on the phase diagram for the given coolant. The locus of such points corresponding to all locations of the phase-transition boundary inside a porous wall is a continuous curve. From the trend of this curve relative to the saturation line, we can draw conclusions concerning the location of the phase-transition boundary and concerning the stability of the system. Only in a stable system can the phase-transition boundary be located inside a porous wall.

The solution scheme becomes even more comprehensive and the results will appear in analytical form, if the physical properties of each coolant phase and of the wall material are assumed constant. This does not diminish the generality of the conclusions concerning the conditions for process stability.

TABLE 1. Physical Properties of Water and Water Vapor on the Saturation Line

$P_s, \text{bar}$	$T_s, ^\circ\text{C}$	$\frac{v''}{v'}$	$\frac{\rho'}{\rho''}$
0,1	48,83	242,0	$1,45 \cdot 10^4$
1,0	99,63	73,5	$1,69 \cdot 10^3$
10,0	179,88	17,7	$1,76 \cdot 10^2$
100,0	310,96	2,91	$1,26 \cdot 10^1$

With a hypothetically fixed location of the phase-transition boundary and assumed constant physical properties of each coolant phase and of the solid wall material, the thermal part of the problem becomes linear. The energy equations (3)-(5) become linear with constant coefficients because, according to (1), the rate of coolant flow is the same through any cross section of the wall. Linear also is the boundary condition (8) regarding the change in thermal flux density at a fixed phase-transition boundary. The energy equations for all three zones can be reduced to a dimensionless form. For this purpose, it is necessary to introduce a dimensionless coordinate  $x = x/\delta$  and dimensionless groups characterizing the process of transpiration cooling:

$$K_0 = \frac{G\delta c'}{\lambda'}, \quad K_1 = \frac{G\delta c'}{\lambda_1}, \quad K_2 = \frac{G\delta c''}{\lambda_2}. \quad (12)$$

A solution of the dimensionless energy equations with the boundary conditions (6)-(9) will yield the same kind of expression for the temperature distribution in each:

$$\theta_0 = \frac{t_0 - T_\infty}{T_0 - T_\infty} = \exp(K_0 x), \quad \theta_1 = \frac{t_1 - T_0}{T_1 - T_0} = \frac{\exp(K_1 x) - 1}{\exp(K_1 l) - 1}, \quad (13)$$

$$\theta_2 = \frac{t_2 - T_l}{T_1 - T_l} = \frac{\exp[K_2(x-l)] - 1}{\exp[K_2(1-l)] - 1}.$$

The dimensionless temperatures have been defined relative to the temperatures at the interzone boundaries:

$$T_0 = T_\infty + \frac{q \{ \exp[K_2(l-1)] - Gr \} \exp(-K_1 l)}{Gc'}, \quad (14)$$

$$T_l = T_\infty + \frac{q \exp[K_2(l-1)] - Gr}{Gc'}, \quad (15)$$

$$T_1 = T_l + \frac{q \{ 1 - \exp[K_2(l-1)] \}}{Gc''}. \quad (16)$$

Expression (15) for the temperature at the hypothetical phase-transition boundary is particularly noteworthy. It will be referred to a few times again in the course of this analysis.

In the only case where it had been possible to actually measure the temperature distribution in a two-layer porous structure of a stable cooling system, close agreement was found with the results of the analytical solution in [6] by a method not much different than the one proposed here. For the purpose of comparison, test values referred to the space coordinate of the phase-transition boundary were used in the calculation.

The pressure at the phase-transition boundary can be found by integrating the flow equation, if the coolant flow rate is known. In a study of two-phase cooling, one usually determines the flow rate from the equation of heat balance at the outer surface [6, 26, 27]. One assumes that the necessary change in the flow rate is ensured by regulation of the feed pressure. Such a method of control is feasible only in stable systems, however. Within the most significant range of flow rates, the hydrodynamic characteristics of an unstable thermotechnical system also have a segment with a negative slope, where control by regulating the pressure drop becomes ineffective [9, 12].

Before specifying some flow rate, we must establish the basic trends of coolant flow with phase transformation inside a porous wall under some constant pressure difference  $P_0 - P_1$  between its surfaces. For this purpose, we integrate the flow equation (2) over the entire wall thickness and take here into account the condition of continuity (1) as well as the constancy of the drag coefficients:

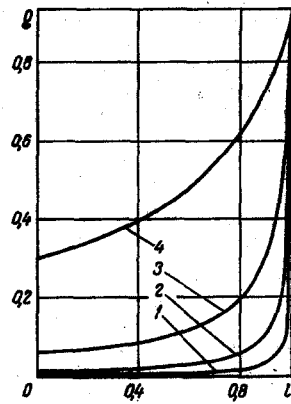


Fig. 2

Fig. 2. Dimensionless mass rate of coolant flow as a function of the location of the phase-transition boundary, at  $Re = 0.1$ : 1)  $P_S = 0.1$  bar; 2)  $P_S = 1$  bar; 3)  $P_S = 10$  bars; 4)  $P_S = 100$  bars.

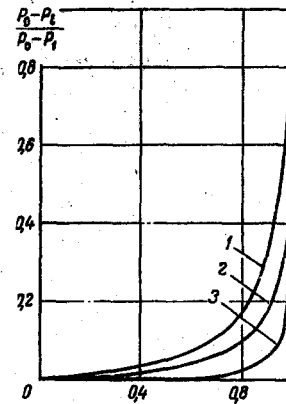


Fig. 3

Fig. 3. Dimensionless pressure at the phase-transition boundary, as a function of the location of this boundary, at  $P_S = 10$  bars: 1)  $Re = 0$ ; 2)  $Re = 1.0$ ; 3)  $Re = \infty$ .

$$P_0 - P_1 = \alpha G \left[ \int_0^L \frac{\mu(X)}{\rho(X)} dX + \int_L^\delta \frac{\mu(X)}{\rho(X)} dX \right] + \beta G^2 \left[ \int_0^L \frac{dX}{\rho(X)} + \int_L^\delta \frac{dX}{\rho(X)} \right] \quad (17)$$

The nonanalytic tabular character of the physical properties of the coolant in either state makes it unfeasible to perform this integration in closed form, especially since the actual distribution of pressure and temperature is still unknown. The process would be very different qualitatively, if the physical properties were assumed constant and corresponding to some value of a governing process parameter. For a cooling system with phase transformation, it seems most appropriate to regard its state corresponding to the ambient pressure  $P_1$  on the saturation line as the reference. Integrating Eq. (17) and then dividing both sides by  $\delta v'$  ( $v' = \mu/\rho'$ ) yields

$$\frac{P_0 - P_1}{\delta v'} = \alpha G \left[ l + \frac{v''}{v'} (1-l) \right] + \frac{\beta G^2}{\mu'} \left[ l + \frac{\rho'}{\rho''} (1-l) \right], \quad (18)$$

where  $l = L/\delta$  is the dimensionless space coordinate of the phase-transition boundary and where the prime (') and the double prime (") refer to the physical properties of the liquid and the vapor, respectively, on the saturation line. The first and the second term inside brackets represent the contribution of the liquid component and the vapor component, respectively, to the viscous drag (first brackets) and to the inertial drag (second brackets). The order of magnitude of these components, assuming the two zones to be of equal lengths ( $l = 1/2$ ), can be estimated from tabulated data [28].

With the appropriate notation

$$m = \left[ l + \frac{v''}{v'} (1-l) \right], \quad n = \left[ l + \frac{\rho'}{\rho''} (1-l) \right], \quad (19)$$

$$G_1 = \frac{P_0 - P_1}{\delta v' \alpha}, \quad Re = \frac{G_1 \beta}{\mu'}$$

we can now conveniently express the flow equation in terms of the dimensionless flow rate  $g = G/G_1$  and the Reynolds number:

$$1 = gm + g^2 n Re. \quad (20)$$

The physical meaning of parameter  $G_1$  is the flow rate of liquid in the Darcy mode, while the Reynolds number may be regarded as measuring the ratio of inertial drag force to viscous drag force during the flow of liquid through a porous wall. The characteristic dimension of a porous structure is then  $\beta/\alpha$ , which represents the ratio of the respective drag coefficients.

After mathematical transformations analogous to the preceding ones, we determine the pressure at the phase-transition boundary according to the expression

$$\frac{P_0 - P_l}{P_0 - P_1} = gl + g^2 l \text{Re}. \quad (21)$$

In order to comprehend the results obtained by the solution of Eqs. (20) and (21), let us consider the example of water filtrating through a plate of stainless steel,  $\delta = 5$  mm thick with a porosity  $\Pi = 20\%$ . The values of the drag coefficients (viscous drag  $\alpha = 3.5 \cdot 10^{13} \text{ m}^{-2}$ , inertial drag  $\beta = 1.2 \cdot 10^8 \text{ m}^{-1}$ ) are taken from the data in [18].

Both the specific rate of coolant flow (solution to Eq. (20)) and the pressure at the phase-transition boundary (21) are functions of the parameters  $l$ ,  $\nu''/\nu'$ ,  $\rho'/\rho''$ ,  $\mu'$ ,  $\gamma'$ , and  $\text{Re}$ . The physical properties of liquid and vapor are uniquely determined by the saturation pressure. The effect of ambient pressure on the relation between the dimensionless mass flow rate and the location of the phase-transition boundary is shown in Fig. 2. The most significant feature of the process is revealed here, namely the sharp decrease in the coolant flow rate during a slight widening of the evaporation zone from the outer surface ( $l = 1$ ) inward while the feed pressure is held constant. It is very difficult to ensure effective control of the flow rate during phase transformation within a thin surface layer under such circumstances. Raising the system pressure will cause the flow rate to vary more smoothly.

The ratios of pressure drops across the liquid zone and the vapor zone respectively during the flow of coolant, according to Eqs. (20) and (21), are shown in Fig. 3 for an ambient pressure of 10 bars. The contribution of the liquid zone to the total drag in the plate is negligible, even when the vapor zone becomes narrower. This trend is more pronounced at higher values of the Reynolds number, which characterizes a transition to an inertial flow mode.

The results obtained here become particularly significant in view of the opposite directions in which the liquid zone and the vapor zone affect the process stability. The viscosity of the liquid decreases, as the temperature rises, while the viscosity of the vapor increases. When a plate is cooled with a one-phase liquid, then a small increase in the heat load will cause the wall temperature to rise and thus the viscosity of the liquid to drop. The drag decreases then and the flow rate increases till equilibrium has been reached. The effect will be opposite in the vapor zone. A small temperature rise causes a drop in the vapor flow rate, which allows the temperature of both vapor and wall to rise further.

With the variability of the physical properties of the coolant taken into account in the integration of the flow equation, the resulting relations must be quantitatively adjusted. Such process peculiarities as the sharp decrease in the flow rate during deeper penetration of the boiling zone, the major contribution of the vapor zone to the total drag in the plate, and the effect of the system pressure as well as of the flow modes become so prominent now as not to be subject any more to any substantial qualitative changes.

Comparing the pressure according to (21) and the temperature according to (15) at the phase-transition boundary, one can see that they are both determined not only by the given system parameters but also by the location of that phase-transition boundary: its space coordinate  $l$  appears in each equation either explicitly, or implicitly in terms of the flow rate  $G(l)$ . This hypothetical coordinate of the phase-transition boundary is then another parameter and can assume all values on the closed interval  $l \in [0, 1]$ . The thus established parametric relation is conveniently written in shorthand:

$$P_l = P_l(T_l). \quad (22)$$

The specific form of this relation is determined by the process parameters. Let us examine a few possible variants at low values of the Reynolds number. We select a plate  $\delta = 5$  mm thick with a porosity  $\Pi = 20\%$  and with drag coefficients which depend on the viscosity according to the data in [18]. Let the ambient pressure be  $P_1 = 10$  bars. The plate is cooled with water so that, with the phase-transition boundary located at  $l = 0.95$ , the Reynolds number is  $\text{Re} = 0.1$  and constant. The necessary pressure drop is found from relation (19) to be  $P_0 - P_1 = 1.25$  bar. The specific flow rate of water is then  $G = 1.9 \text{ kg/m}^2 \cdot \text{sec}$  and the pressure drop across the liquid zone is found from relation (21) to be  $P_0 - P_1 = 0.433(P_0 - P_1)$ . The pressure  $P_S = 10.7$  bars at the phase-transition boundary corresponds to a saturation temperature  $T_S = 182.8^\circ\text{C}$ .

We now consider three variants with different loading thermal flux densities:  $q_1 = 3.5 \cdot 10^7 \text{ W/m}^2$ ,  $q_2 = 1.8 \cdot 10^7 \text{ W/m}^2$ , and  $q_3 = 0.83 \cdot 10^6 \text{ W/m}^2$ . The effective thermal conductivity of the vapor-(porous)solid system, with which the phase-transition boundary located at  $l = 0.95$  will be in equilibrium, is found from

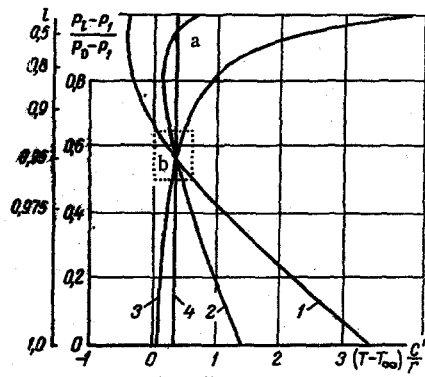


Fig. 4

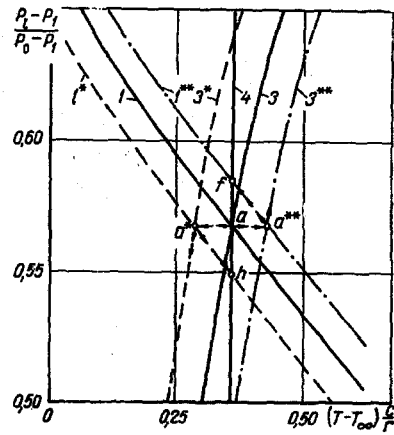


Fig. 5

Fig. 4. Pressure as a function of the temperature, at the phase-transition boundary in the three systems: 1)  $q = 3.5 \cdot 10^7 \text{ W/m}^2$  and  $\lambda_2 = 0.65 \text{ W/m} \cdot ^\circ\text{C}$ ; 2)  $q = 1.8 \cdot 10^7 \text{ W/m}^2$  and  $\lambda_2 = 1.0 \text{ W/m} \cdot ^\circ\text{C}$ ; 3)  $q = 0.83 \cdot 10^7 \text{ W/m}^2$  and  $\lambda_2 = 2.6 \text{ W/m} \cdot ^\circ\text{C}$ ; 4) saturation line.

Fig. 5. Blown up portion of Fig. 4: solid lines 1 and 3 represent a quiescent state, dashed lines represent a state under a slightly decreasing heat load, dashed-dotted lines represent a state under an increasing heat load.

Eq. (15) for  $T_l = T_s = 182.8^\circ\text{C}$  to be  $\lambda_{2,1} = 0.65 \text{ W/m} \cdot ^\circ\text{C}$ ,  $\lambda_{2,2} = 1.0 \text{ W/m} \cdot ^\circ\text{C}$ , and  $\lambda_{2,3} = 2.6 \text{ W/m} \cdot ^\circ\text{C}$  respectively.

The temperature—pressure relation in the hypothetical zone of phase transformation is shown in Fig. 4 for the three variants. One coordinate here is the dimensionless pressure at the phase-transition boundary, determined according to Eq. (21). For comprehensiveness, we have also shown here the corresponding dimensionless space coordinate of the phase-transition boundary. The relation between this dimensionless space coordinate and the dimensionless pressure remains the same for all the three modes considered here. The other coordinate is the dimensionless temperature. It is convenient to represent the temperature at the phase-transition boundary in this way, because expression (15) can then be reduced to

$$(T_l - T_\infty) \frac{c'}{r} = \frac{q \exp [K_2(l-1)]}{Gr} - 1. \quad (23)$$

In referred coordinates, the saturation line 4 becomes almost vertical: a pressure drop across the plate  $P_0 - P_1 = 1.25 \text{ bar}$  at  $P_1 = 10 \text{ bars}$  corresponds to a change in the saturation temperature  $\Delta T_s = 5.2^\circ\text{C}$ , or  $\Delta T_s(c'/r) = 0.011$  in dimensionless coordinates.

All three curves intersect the saturation line at one point, but their slopes at this point and their trends beyond it are different. Furthermore, according to curve 2, in the second mode the phase transition boundary may be located not only at  $l = 0.95$  (point  $a$ ) but also at  $l = 0.4$  (point  $b$ ).

In order to locate the phase-transition boundary without ambiguity, we establish a relation between the stability of the system and the mode of intersection of the pressure—temperature curve with the saturation line within the zone of phase transformation. Let the loading thermal flux density on systems 1 and 3 drop suddenly by a small amount (by 5% of the initial level). Under the new steady-state conditions, then, the temperature in the hypothetical phase-transformation zone drops also and assumes values represented by the dashed lines 1\* and 3\* respectively in Fig. 5. At the instant when the thermal flux density changes, the liquid—vapor interface is located at point  $a$ . As the heat load decreases, the amount of heat input to the phase-transformation zone becomes insufficient for complete evaporation. If the liquid had evaporated completely, then the temperature in the evaporation zone tentatively represented by point  $a^*$  would have been below the saturation point  $a$ . The phase-transition boundary moves, therefore, toward the outer surface of the plate and this is accompanied by an increase in the coolant flow rate (curve 3 in Fig. 2 gives an indication about the change in the coolant flow rate in the three cases considered here). The subsequent trend of the process is determined from the mode of intersection between curves 1 or 3 and the saturation line at point  $a$ .

It follows from Eq. (16) written as

$$q \exp [K_2(l-1)] = q - Gc''(T_1 - T_l), \quad (24)$$

that the numerator in the first term on the right-hand side of Eq. (23) for the temperature at the hypothetical phase-transition boundary represents the thermal flux density at this boundary.

If the displacement of the phase-transition boundary is accompanied by an increase in the heat load on it which is faster than the increase in the heat necessary for evaporating the fast increasing coolant mass (denominator on the right-hand side of Eq. (23)), then the temperature at the hypothetical phase-transition boundary will increase and a new steady state will be established with an equilibrium mode of phase transformation. The phase-transition boundary in system 1 will move by a small distance to a new location at an equilibrium temperature represented by point h. The temperature change in the evaporation zone during this transition to the new state is tentatively represented by the line  $a-a^*-h$ .

The amount of heat load on the moving phase-transition boundary in system 3 increases slower than the amount of heat necessary for evaporating the fast increasing coolant mass. The phase-transition boundary will move all the way to the outer surface of the plate. The coolant flow rate now exceeds the flow rate based on complete evaporation.

If the thermal flux density increases by a small amount, then the phase-transition boundary in system 1 moves deeper inward to a new location. The equilibrium temperature of phase transformation is represented here by point f. In system 3, on the other hand, a small increase in the density of the loading thermal flux will cause a continuous displacement of the phase-transition boundary toward the inner surface of the plate. During boiling much more vapor appears at the inner surface than is transmitted through the plate.

The system can also be dislodged from its initial state by small fluctuations of the ambient pressure or the feed pressure.

The mode of intersection between curve 1 and the saturation line characterizes a stable system of two-phase transpiration cooling where a small perturbation of the process parameters causes a transition to a new stable state near the original one. In system 3, a small such perturbation causes a transition to a new state much different from the original one. System 3 is unstable.

Considering that during evaporation  $dP_s/dT_s > 0$ , we may formulate the stability criterion as follows: in order that a process of two-phase transpiration cooling be stable, it is necessary that the tangent to the pressure-temperature curve at the hypothetical phase-transition boundary be steeper than the tangent to the saturation line at the operating point. This can be stated mathematically as

$$\frac{dP_l}{dT_l} > \frac{dP_s}{dT_s}, \quad \text{if} \quad \frac{dP_l}{dT_l} > 0; \quad \frac{dP_s}{dT_s} > \frac{dP_l}{dT_l}, \quad \text{if} \quad \frac{dP_l}{dT_l} < 0. \quad (25)$$

From the relations derived here, it is possible to find the range of parameter values within which a stable performance of a two-phase transpiration cooling system is ensured.

#### NOTATION

X	is a dimensional space coordinate;
x	is a dimensionless space coordinate;
G	is the dimensional flow rate of coolant;
g	is the dimensionless flow rate of coolant;
L	is the dimensional space coordinate of the phase-transition boundary;
l	is the dimensionless space coordinate of the phase-transition boundary;
$\delta$	is the plate thickness;
$P_0$	is the feed pressure;
$P_1$	is the ambient pressure;
q	is the loading thermal flux density;
$\alpha$	is the coefficient of viscous drag;
$\beta$	is the coefficient of inertial drag;
$T_\infty, T_0, T_1$	are the temperatures at the characteristic surfaces;
$\theta_0, \theta_1, \theta_2$	are the dimensionless temperatures;
$\Pi$	is the porosity of the wall material;



- $\lambda$  is the thermal conductivity;  
 $\mu$  is the dynamic viscosity;  
 $\nu$  is the kinematic viscosity;  
 $\rho$  is the density;  
 $c$  is the specific heat;  
 $r$  is the total heat of evaporation;  
 $G_1$  is the specific rate of coolant flow in the Darcy mode;  
 $Re$  is the Reynolds number.

### Subscripts and Superscripts

- $s$  refers to the saturation line;  
 $l$  refers to values of parameters at the hypothetical phase-transition boundary;  
 $M$  refers to the plate material;  
 $(')$  refers to the physical properties of the liquid on the saturation line;  
 $('' )$  refers to the physical properties of the vapor on the saturation line.

### LITERATURE CITED

1. P. Duwez and H. L. Wheeler, *J. Aeronaut. Sci.*, **15**, No. 9, 509-521 (1948).
2. V. M. Polyayev and A. V. Sukhov, *Teplofiz. Vys. Temp.*, **7**, No. 5, 1037-1039 (1969).
3. A. V. Gomez, D. M. Curry, and C. G. Johnston, *AIAA Paper No. 71-445* (1971).
4. R. Reth and W. Frost, *AIAA Paper No. 25-72* (1972).
5. P. C. Wayner and S. G. Bankoff, *J. AIChE*, **11**, No. 1, 59-64 (1965).
6. J. C. Y. Koh and E. P. delCasal, in: *Developments in Mechanics*, **4**, 1527-1541 (1968).
7. J. C. Y. Koh, C. Jaeck, B. Benson, and B. Causineau, *AIAA Paper No. 70-151* (1970).
8. V. K. Pai and S. G. Bankoff, *J. AIChE*, **12**, No. 4, 727-736 (1966).
9. P. A. Petrov, *Hydrodynamics of a Parallel-Flow Boiler* [in Russian], Gosénergoizdat, Moscow (1960).
10. I. I. Morozov and V. A. Gerliga, *Stability of Boilers* [in Russian], Atomizdat, Moscow (1969).
11. L. S. Tong, *Heat Transfer during Boiling and Two-Phase Flow* [Russian translation], Izd. Mir, Moscow (1969).
12. J. A. Boure, A. E. Bergles, and L. S. Tong, *ASME Paper No. 71-HT-68* (1971).
13. V. E. Doroshchuk, *Critical Modes of Heat Transfer in Pipes with Boiling Water* [in Russian], Izd. Énergiya, Moscow (1970).
14. Ya. A. Kaminskii, *Poroshk. Metallurg.*, No. 8, 53-61 (1965).
15. R. R. Kunz, L. S. Langston, B. H. Hilton, S. S. Wyde, and G. H. Mashick, *NASA Report CR-812* (1967).
16. S. V. Belov et al., *Khim. i Neft. Mashinostroenie*, No. 11, 13-14 (1971).
17. J. Heberlin and E. Pfender, *Trans. ASME, Heat Transmission*, **93C**, No. 2, 17-25 (1971).
18. I. M. Fedorochenko et al., *Poroshk. Metallurg.*, No. 12, 52-57 (1967).
19. L. Green Jr. and P. Duwez, *J. Appl. Mechan.*, **18**, No. 1, 39-45 (1951).
20. Yu. V. Il'in, *Izv. VUZov, Aviats. Tekh.*, No. 1, 65-73 (1959).
21. S. V. Belov et al., *Poroshk. Metallurg.*, No. 1, 71-75 (1972).
22. Yu. P. Kukota et al., *Poroshk. Metallurg.*, No. 11, 32-40 (1965).
23. A. P. Dubrovskii and P. A. Isaev, *Poroshk. Metallurg.*, No. 1, 46-49 (1966).
24. A. F. Chudnovskii, *Thermophysical Properties of Disperse Materials* [in Russian], Fizmatgiz, Moscow (1962).
25. W. Frost, R. Reth, and W. T. Buchanan, *AIAA Paper No. 72-24* (1972).
26. J. W. Yang, *J. Spacecraft and Rockets*, **6**, No. 6, 759-762 (1969).
27. V. P. Popov and A. I. Shoikhet, in: *Thermoaerodynamics* [in Russian], Izd. Nauka i Tekhnika, Minsk (1970), pp. 17-26.
28. M. P. Bukalovich, S. L. Rivkin, and A. A. Aleksandrov, *Thermophysical Tables for Water and Steam* [in Russian], Izd. Standartov, Moscow (1969).